THREE-DIMENSIONAL THEORY OF THE SMITH-PURCELL FREE-ELECTRON LASER

J. D. Jarvis and H. L. Andrews,
Department of Physics and Astronomy, Vanderbilt University, Nashville, TN 37235, U.S.A.

Abstract

We present an analytic theory for the exponential-gain (growth) regime of a Smith-Purcell free-electron laser amplifier (oscillator), which includes the effects of transverse diffraction in the optical beam. The optical mode is guided by the electron beam, having a mode width that depends upon the gain length. For the case of a wide electron beam, the dispersion relation converges with that of the 2-D theory. When the electron beam is narrow, the conventional cubic-dispersion relation is replaced by a five-halves dispersion. The dispersive properties of the grating divide device operation into four distinct regions, two amplifier and two oscillator. The number and location of physically allowed roots changes depending on operating region. Additionally, in the narrow-beam case, new challenges arise in satisfying the boundary conditions required for operation as an oscillator

INTRODUCTION

The wide range of potential applications for THz radiation is currently driving interest in the development of intense, compact, tunable THz sources. Such applications include: resonant excitation and spectral analysis of chemical and biological molecules and systems, medical and industrial imaging, and investigations in materials science and nanostructures [1,2]. Electron-beam-based devices are very promising sources of THz radiation. These include synchrotrons, conventional FELs, and slow-wave devices, such as backward-wave oscillators. While synchrotrons and conventional FELs are large and expensive, slow-wave devices can be compact, laboratory-scale instruments.

Slow-wave structures support subluminal electromagnetic modes, which may interact resonantly with an electron beam passing in close proximity. This resonant interaction causes bunching in the electron beam and amplitude growth of an evanescent optical field. For an open-grating structure, superradiant Smith-Purcell radiation may be extracted at harmonics of the evanescent wave [3]. This configuration is known as a Smith-Purcell free-electron laser (SPFEL). The SPFEL may be operated as an amplifier (convective instability), or as an oscillator (absolute instability), depending on the sign of the laser wave's group velocity. The two-dimensional theory of such a device has been examined in detail for the exponential gain/growth regime [4,5,6,7], and is closely supported by PIC simulations [6,8,9]. A two-dimensional numerical treatment of device operation from startup to saturation, with one-dimensional electron dynamics, has also been performed [7].

In this work, we include the effects of transverse diffraction in the optical beam of an SPFEL. The approach used is similar to that used for the 3-D theory of the Cerenkov FEL [10]. As expected, three-dimensional effects increase the gain length and oscillator start current substantially. Furthermore, compared to the 2-D theory, their dependence on the beam current increases due to gain guiding. We find that diffraction of the optical beam in the periodic-grating structure subdivides device operation into two amplifier regions and two oscillator regions. For the amplifier and oscillator regions furthest from the Bragg point, we find the inclusion of a fast wave in the physically allowed solutions. This is very surprising, considering the nature of a guided system. For the oscillator region closest to the Bragg point there are only two physically allowed solutions. It is not known how the required boundary conditions on the electron and optical beams can be satisfied in this region.

DISPERSION

In an SPFEL, resonant energy exchange between the electron beam and bound surface modes gives rise to spatial modulations in the beam density. These density modulations lead to superradiant enhancement of the emitted SP radiation, and subsequent modification of its angular distribution [3]. In the following analysis we calculate the fields subject to the Maxwell equations and boundary conditions and solve for the dispersion relation. We then introduce the electron beam as a perturbation and calculate the resulting wavenumber and frequency shifts for solutions to the dispersion relation.

Table 1: Dartmouth grating and beam parameters

Grating period	173 μm
Groove width	62 μm
Groove depth	100 μm
Grating length	12.7mm
E-beam width/height	60 μm
E-beam current	1 mA
E-beam height above grating (measured from bottom of beam)	0 μm

For an electron beam energy of $150\ \mathrm{kV}$ and the grating parameters of Table 1, the intensity scale height of the evanescent wave is $\Delta x = \beta\gamma\lambda / 4\pi \approx 38\ \mu\mathrm{m}$, where $\beta \sim 0.43$ is the normalized electron velocity,

$\gamma = 1/\sqrt{1-\beta^2}$, and $\lambda \sim 10^{-3}$ m is the free-space wavelength. We anticipate from simple diffraction arguments that the transverse mode width is of order $\Delta y \approx \sqrt{\beta\lambda Z_g / 2\pi}$ (~millimeters), where Z_g (~centimeters) is the gain length. Schematics of the device geometry with all pertinent dimensions are given in Figures 1 and 2.

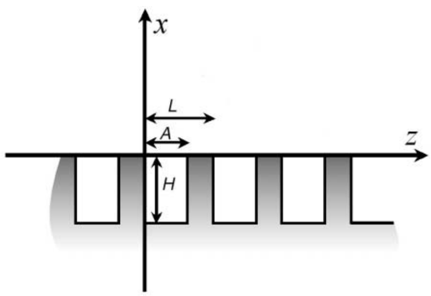

Fig. 1 Geometry of grating structure, viewed from the side

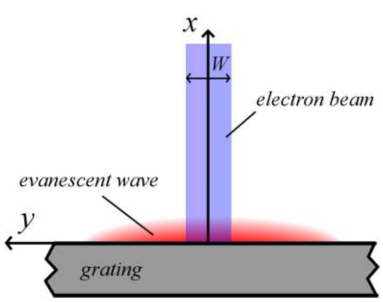

Fig. 2 Geometry of evanescent wave and electron beam, viewed from front

Because the fields vanish exponentially above the scale height, we simplify the theory by allowing the electron beam to extend to infinity in the x direction. A filling factor can be used to correct for errors introduced by this approximation [6,11]

To calculate the dispersion relation for the grating, in the absence of the electron beam, we expand the field above the grating in Floquet series and the field in the grooves as Fourier series. Invoking the Maxwell equations and matching the fields at the grating surface, we arrive at the empty grating dispersion function $D\left(\omega, k, k_y^{\,2}\right)$, where ω is the frequency, k is the longitudinal wavenumber, and k_y is the wavenumber in the y direction. We then expand the dispersion function about the synchronous point ($\omega_0 = \beta c k_0$) in ω, k, and $k_y^{\,2}$, introducing the electron beam as a perturbation. In the limit where the electron beam is infinitely wide the dispersion relation matches the 2-D theory [5]. For the case of a very narrow beam the resulting dispersion relation is

$$\left(\delta\omega - \beta c\delta k\right)^2 \left[\frac{D_\omega}{D_y}\left(\delta\omega - \beta_g c\delta k\right)\right]^{\frac{1}{2}} = \Delta \qquad (1)$$

where β_g is the evanescent wave's goup velocity, $\delta\omega$ and δk are the complex frequency and wavenumber shifts respectively, D_ω and D_y are partial derivatives of the no-beam dispersion function with respect to ω and $k_y^{\,2}$, and

$$\Delta = \frac{\beta^3 c^2 W}{ALD_y}\frac{\omega_e^{\,2}}{\gamma^2\omega_0^{\,2}}\tan\left(\frac{\omega_0}{c}H\right)\left[1-\cos\left(k_0 A\right)\right]. \quad (2)$$

Calculations show that D_ω is negative, irrespective of k, but D_y changes such that $D_y > 0$ near the center of the Brillouin zone $\left(k/K = 1/2\right)$ and $D_y < 0$ towards the edges of the zone $\left(k = 0, K\right)$. This subdivides operation of the SPFEL into the four distinct regions pictured in Figure 3 with the dispersion relation. Some roots are eliminated in each region of operation because they do not allow the fields to vanish at $y = \pm\infty$. A diagram detailing this selection is given in Figure 4. We now consider the amplifier and oscillator regimes of the SPFEL.

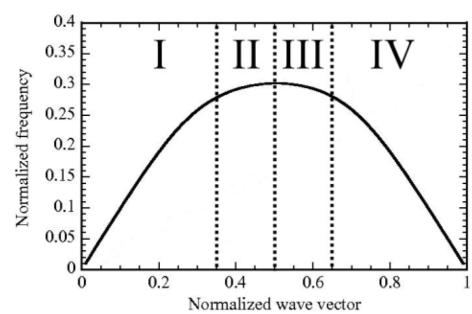

Fig. 3 Dispersion relation with different regions of operation

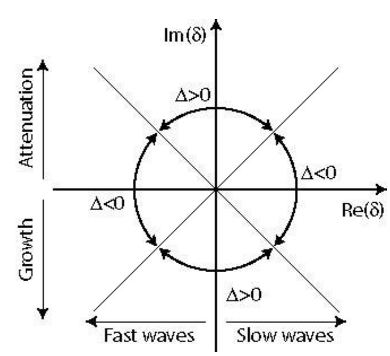

Fig. 4 Diagram for selection of allowed roots

AMPLIFIER

When the device operates as a steady-state amplifier, $\delta\omega = 0$ and β_g is positive. In region II, the roots of the dispersion relation are

$$\delta k_n = \Gamma^{\frac{2}{5}} e^{i\frac{4}{5}n\pi} \tag{5}$$

where

$$\Gamma = \frac{1}{\beta^2 c^2}\left|\frac{D_y \Delta}{D_\omega \beta_g c}\right|^{\frac{1}{2}}. \tag{6}$$

Similarly, in region I the roots are

$$\delta k_n = \Gamma^{\frac{2}{5}} e^{i\left(\frac{4}{5}n\pi + \frac{\pi}{5}\right)}. \tag{7}$$

In region II only two roots are physically allowed, $n = 2,3$. From Figure 5 we see that these are slow waves, i.e. they have a phase velocity lower than that of the no-beam-operating point.

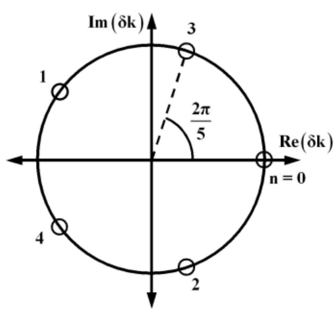

Fig. 5 Roots for region II in the complex plane

In region I, however, there are three physically allowed roots including one fast wave solution. It is surprising that a fast wave is allowed in a gain-guided system. In region II, the $n = 3$ root has loss and the $n = 2$ root has gain. The gain for the $n = 2$ root is given by

$$\mu_{3D} = -\mathrm{Im}\left(\delta k_2\right) = \Gamma^{\frac{2}{5}} \sin\left(\frac{2}{5}\pi\right) \tag{8}$$

and has a corresponding $1/e$ optical mode width of

$$\Delta y = 2\left(\left|\frac{D_\omega}{D_y}\beta_g\right| c\right)^{-\frac{1}{2}} \Gamma^{-\frac{1}{5}} \cos\left(\frac{\pi}{5}\right). \tag{9}$$

The relationship given in (9) is simply understood to be the manifestation of gain guiding in the SPFEL. As an example, we consider the grating and beam described in Table 1. The three-dimensional gain is plotted in Figure 6, along with the two-dimensional gain, which has been scaled down by a factor of three to appear on the same graph.

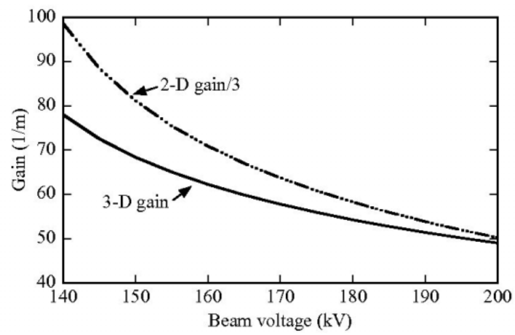

Fig. 6 Computed gain for 2-D and 3-D theories as a function of beam voltage

The transverse profile of the electric field is given in Figure 7, and the $1/e$ mode width is found to be $\Delta y \approx 4.4\mathrm{mm}$. By examining the geometry of this mode, it is clear that the initial assumptions made concerning its dimensions are justified

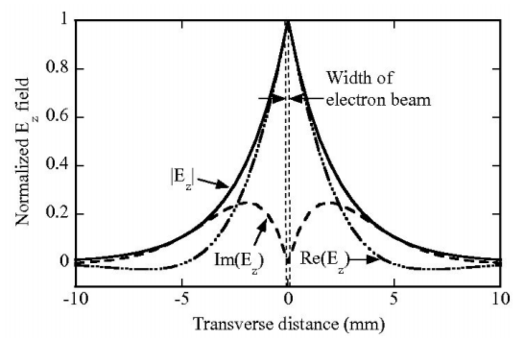

Fig. 7 Transverse profile of the electric-field strength

OSCILLATOR

In regions III and IV the group velocity of the evanescent mode is negative. This allows information about the bunching of the electron beam at the grating exit to be carried back upstream. This serves as an intrinsic form of feedback and, provided that the beam current exceeds the so-called start current, allows the device to oscillate. For a solution to exist in the oscillator case, three boundary conditions must be satisfied in conjunction with the dispersion relation (1). The electron beam must be free of density and velocity modulations at the upstream end of the grating, and the input optical field at the downstream end must vanish [5,6]. These boundary conditions are satisfied by interference of the three waves that compose the mode. Solutions to the inhomogeneous system can have different transverse widths due to the presence of gain guiding. Therefore, if only inhomogeneous solutions are used, the boundary condition on the input field cannot be satisfied for all y. For a general solution to the system, arbitrary amounts of the homogeneous solutions may be added. In the following analysis we require that the boundary conditions be satisfied only on the beam axis. We find that while region IV has three physically allowed roots, only two waves are admitted in region III. It is not clear how all three boundary conditions may be satisfied without the presence of a third wave. We therefore restrict our analysis of the oscillator regime to region IV.

To form a mode of the oscillator, each wave must have the same frequency shift $\delta\omega$. The boundary conditions are defined by

$$\begin{vmatrix} 1/\delta_1^{\,2} & 1/\delta_2^{\,2} & 1/\delta_3^{\,2} \\ 1/\delta_1 & 1/\delta_2 & 1/\delta_3 \\ e^{i\xi\delta_1} & e^{i\xi\delta_2} & e^{i\xi\delta_3} \end{vmatrix} = 0 \qquad (10)$$

where δ_j and ξ are dimensionless variables given by

$$\delta_j = \left[\frac{\beta^2 c^{\frac{5}{2}} \left|\beta_g\right|^{\frac{1}{2}}}{\Delta}\left(\frac{D_\omega}{D_y}\right)^{\frac{1}{2}}\right]^{\frac{2}{5}} \left(\delta k_j - \frac{1}{\beta c}\delta\omega\right), \qquad (11)$$

$$\xi = \left[\frac{\Delta}{\beta^2 c^{\frac{5}{2}} \left|\beta_g\right|^{\frac{1}{2}}}\left(\frac{D_y}{D_\omega}\right)^{\frac{1}{2}}\right]^{\frac{2}{5}} Z\,. \qquad (12)$$

To find the start current we require $\mathrm{Im}\left[\kappa\left(\xi_0\right)\right] = 0$, where

$$\kappa = -\left[\frac{\beta^2 \left|\beta_g\right|^{\frac{1}{2}}}{\Delta}\left(\frac{D_\omega}{D_y}\right)^{\frac{1}{2}}\right]^{\frac{2}{5}} \left(\frac{1}{\left|\beta_g\right|} + \frac{1}{\beta}\right)\delta\omega \qquad (13)$$

and solve the dispersion relation

$$\delta_j^{\,2}\sqrt{\delta_j - \kappa} \pm 1 = 0 \qquad (14)$$

subject to (10). The lowest dimensionless root found is $\xi_0 = 1.194$, $\kappa\left(\xi_0\right) = 1.802$. Both the 2-D and 3-D start currents are plotted as a function of operating voltage in Figure 8.

CONCLUSIONS

We have presented a three-dimensional theory of SPFEL oscillator (amplifier) operation for the exponential growth (gain) regime. We find that 3-D effects substantially increase both gain length (amplifier) and start current (oscillator). Unexpected consequences result from inclusion of diffraction in the grating's periodic structure. Device operation is divided into four regions, which are characterized by the number and location of physically allowed roots to the dispersion relation. Fast waves are included in some regions of operation despite the guided nature of the interaction. In the present theory the mode width vanishes mathematically at the boundaries of these regions $\left(D_y \to 0\right)$. These consequences are not fully understood at present.

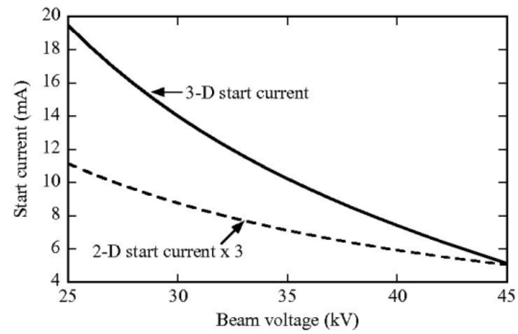

Fig. 8 Oscillator start current as a function of electron beam voltage

ACKNOWLEDGEMENTS

The authors gratefully acknowledge helpful discussions with C. A. Brau and K.-J. Kim. This work was supported by the Medical Free Electron Laser Program of the Department of Defense under grant number F49620-01-1-0429.

REFERENCES

[1] S. P. Mickan and X.-C. Zhang, Int. J. High-Speed Electron. and Sys. **13**, 601 (2003).

[2] P. H. Siegel, IEEE Trans. Microwave Theory and Techniques **50**, 910 (2002).

[3] H. L. Andrews, C. H. Boulware, C. A. Brau, and J. D. Jarvis, Phys. Rev. ST-AB **8**, 110702 (2005).

[4] H. L. Andrews, C. A. Brau, Phys. Rev. ST-AB **7**, 070701 (2004).

[5] H. L. Andrews, C. H. Boulware, C. A. Brau, and J. D. Jarvis, Phys. Rev. ST-AB **8**, 050703 (2005).

[6] H. L. Andrews, C. H. Boulware, C. A. Brau, J. T. Donohue, J. Gardelle, and J. D. Jarvis, New J. Phys. **8** (2006) 289.

[7] V. Kumar and K. J. Kim, Phys. Rev. E **73**, 026501 (2006)

[8] D. Li, Z. Yang, K. Imasaki, and Gun-Sik Park, Phys. Rev. ST-AB **9**, 040701 (2006).

[9] J. T. Donohue and J. Gardelle, Phys. Rev. ST_AB **8**, 060702 (2005).

[10] H. L. Andrews and C. A. Brau, J. Appl. Phys. **101**, 104904 (2007)

[11] G. F. Mkrtchian, Phys. Rev. ST-AB **10**, 080701 (2007)